Received 26 October 2018; revised 30 November 2018; accepted 23 December 2018. Date of publication 27 December 2018; date of current version 1 March 2019. The review of this paper was arranged by Editor A. G. U. Perera.

Digital Object Identifier 10.1109/JEDS.2018.2889888

Au Nanoparticles-Decorated Surface Plasmon Enhanced ZnO Nanorods Ultraviolet Photodetector on Flexible Transparent Mica Substrate

HAINAN ZHANG [1,2], YUNFEI ZHAO[1,2], XIANGSHUN GENG[1,2], YAO HUANG[1,2], YUXING LI [1,2], HOUFANG LIU[1,2], YU LIU [1,2], YUTAO LI[1,2], XUEFENG WANG[1,2], HE TIAN [1,2], RENRONG LIANG [1,2], AND TIAN-LING REN [1,2] (Senior Member, IEEE)

1 Institute of Microelectronics, Tsinghua University, Beijing 100084, China
2 Beijing National Research Center for Information Science and Technology, Tsinghua University, Beijing 100084, China

CORRESPONDING AUTHORS: R. LIANG AND T.-L. REN (e-mail: liangrr@tsinghua.edu.cn; rentl@tsinghua.edu.cn)

This work was supported in part by the National Key Research and Development Program under Grant 2016YFA0200400 and Grant 2016YFA0200300, in part by the National Natural Science Foundation under Grant 61574083 and Grant 61434001, in part by the National Basic Research Program under Grant 2015CB352101, in part by the Special Fund for Agroscientific Research in the Public Interest of China under Grant 201303107, in part by the Research Fund from Beijing Innovation Center for Future Chip, in part by the Independent Research Program of Tsinghua University under Grant 2014Z01006, and in part by the Shenzhen Science and Technology Program under Grant JCYJ20150831192224146.
This paper has supplementary downloadable material available at http://ieeexplore.ieee.org, provided by the author.

ABSTRACT An ultraviolet (UV) photodetector based on hydrothermally processed ZnO nanorods (ZnO NRs) decorated by gold nanoparticles (Au NPs) was demonstrated to exhibit extraordinary optoelectronic properties. Due the implementation of Au NPs, the UV responsivity and specific detectivity reached 70 A/W and 3.41×10^{12} cm $Hz^{1/2}$ W^{-1}, respectively, which were enhanced by approximately four times at an excitation wavelength of 365 nm compared with those of pristine ZnO NRs. Moreover, such photodetector shows good flexibility as well due to the mica substrate, which maintains almost constant performances under different bending radii of curvature and repeatable bending test more than 200 cycles. The photodetector also exhibits good transparency, giving it the potential of integration with other light photodetectors. In addition, a schematic band-diagram and the accompanying finite-difference time-domain analysis were performed to reveal the electron transfer and electric field distribution of ZnO NRs decorated with Au NPs. Our results revealed that the noble metal modified plasmon-enhanced ZnO NRs photodetector with high responsivity, low cost has a great potential for application in manufacturing flexible and transparent integrated optoelectronics.

INDEX TERMS ZnO nanorods, Au nanoparticles, ultraviolet photodetector, mica substrate, flexible bending.

I. INTRODUCTION

Over the past few decades, UV photodetectors have gained more and more attention from academia due to their wide potential applications in many fields, including flame detection, missile plume detection, radiation detection and space communication [1]–[4]. In general, specific qualities of the photodetector, such as responsivity, specific detectivity, reliability and cost are needed to be taken in to account. In most cases, ZnO materials have a large bandgap of about 3.37 eV and it also has good thermal and mechanical stabilities at room temperature. Therefore, wurtzite ZnO is considered to be one of the most ideal materials for UV photodetection. However, the quality of ZnO NRs prepared by hydrothermal method is often not good and usually there are so many defects and impurities distributed on their surface [5], [6]. These defects and impurities can induce defect-related emission and these negative effects will eventually lead to a reduced responsivity of the photodetector. Therefore,

suppressing the defect-related emission while increasing the UV emission is an extremely important issue for the application of ZnO NRs in UV photodetection. This problem can be solved to some extent by using dielectric materials such as Al_2O_3 [7], [8], MgO [5] and so forth to passivate ZnO NRs. However, this passivation process is very complicated and the introduction of dielectric materials will have a negative impact for the post-processing of devices.

In recent years, plasmonic effect of noble metal particles has received extensive attention and it was shown to be an effective method to achieve defect passivation for enhancing optoelectronic device performance. Covering the surface of the semiconductor film or nanostructure with noble metal particles is a simple and effective way to observe plasmonic effect and this method can enhance the electrical and optical properties of semiconductor [9]–[11]. Plasmonic nanoparticles can enhance the electric field of the incident light by several orders of magnitude through plasmonic resonance at their resonant wavelengths. For example, for noble metal nanoparticles such as Al, Ag and Pt, their resonance wavelengths are close to the UV band of ZnO. But for Au NPs, the local surface plasmon resonance (LSPR) is far from UV band but is consistent with the defect emission peak of ZnO in the visible region [12]–[16]. Qin *et al.* [17] reported an enhanced ZnO UV lasing induced by extra green light with Au surface plasmons, which not only confirms the surface plasmon resonance-assisted electron transfer process but also offers an approach to improve the intrinsic UV emission even for heavily defected ZnO through visible light excitation. From the above, one of the unique features of plasmonic noble metal nanoparticles is their capability to enhance the electric field intensity of incident light, thereby opening up a new path for the application of ZnO in many fields such as optical antennas, photocatalysis, spectroscopy and photodetection [10], [11].

In this work, a Au NPs-decorated surface plasmon enhanced ZnO NRs UV photodetector based on flexible transparent mica substrate was designed and fabricated. The UV photoelectric properties and flexible characteristics of the device were systematically analyzed. In addition, FDTD analysis were performed to reveal the electron transfer and electric field distribution of ZnO NRs decorated with Au NPs. When the device was irradiated by light, the oscillating electric field of the incident light would induce LSPR of the Au NPs, which would in turn enhance the UV emission efficiency of semiconductor materials and eventually improve the responsivity of the photodetector.

II. EXPERIMENTAL DETAILS

A. DEVICE FABRICATION AND PHOTORESPONSE MEASUREMENTS

All chemicals used in this work were of analytical grade and were not further purified. ZnO NRs were grown on the mica substrate by a hydrothermal method. Here, the mica substrate was covered with a thin layer of ZnO which was used as a buffer layer. The whole process of the device fabrication was roughly divided into several parts. Firstly, the mica substrate was cleaned sequentially with acetone, isopropanol, alcohol and dried in a nitrogen atmosphere. Secondly, a ZnO seed layer was deposited on the mica substrate by magnetron sputtering using a high purity ZnO target. Subsequently, the ZnO seed layer was annealed under nitrogen atmosphere at 300 °C. The 50 nm thick Au film was deposited on the ZnO seed layer using standard metal lift-off procedure with an interdigital shadow mask to form electron contacts. The interdigital shadow mask was designed using 40 μm width and 250 μm length with a neighboring finger spacing of 40 μm. Standard 1:1 contact photolithography processing was used for this step and the effective area of the photodetector is 0.00222 cm^2. Then equimolar Hexamethylenetetramine (HMTA) ($C_6H_{12}N_4$) and zinc nitrate hexahydrate (Zn $(NO_3)_2{\cdot}(6H_2O)$ were used as solute and they were separately dissolved in deionized water under a magnetic stirrer and finally mixed. Then, the substrate was placed in a beaker containing the mixed solution. The baker was sealed and heated in an oven at 90 °C for 150 minutes. After the heating process, the sample was cleaned with deionized water and dried naturally. Finally, Au NPs solution with 10 nm diameter was sprayed onto the substrate and was dried in air at room temperature. The spraying process is demonstrated in Fig. S1 in the supplementary material. The UV photoresponses of photodetectors were measured using 365 nm wavelength of the illumination source at different illumination intensities. The photoresponses were recorded using a semiconductor device analyzer (Agilent B1500A) during the UV illumination.

B. CHARACTERIZATION

The surface morphology of the samples was characterized by scanning electron microscopy (SEM, Carl Zeiss Microscopy, Merlin). The crystal structure of the samples was examined by X-ray diffraction (XRD, Bruker D8). Furthermore, the optical analysis was performed by UV-Vis spectroscopy (Shimadzu UV-2450) and photoluminescence techniques (PL, Horiba HR800).

C. SIMULATION DETAILS

The electric field distribution of Au NPs located on ZnO NRs was simulated with FDTD method. During the simulation, the shapes of ZnO NRs were set as hexagonal prisms with a height of 800 nm and an edge length of 70 nm in width. The refractive index of ZnO NRs was set as 1.6. Two simulations were conducted regarding different positions of Au NPs on the ZnO NRs. In the first one, two Au NPs were placed on one of the sidewalls and in the second one, two Au NPs were on the top surface. A plane wave with a wavelength ranging from 450 to 650 nm were set as the light source. The boundary condition of perfectly matched layer (PML) was used along the z direction, and periodic boundary condition was used along the x and y direction.

III. RESULTS AND DISCUSSION

Fig. 1(a) and (b) show the schematics and optical image of the prepared device respectively, indicating that both the flexible mica substrate and the final devices have good transparency. Typical field emission scanning electron microscope (FESEM) image of Au NPs decorated ZnO NRs is shown in Fig. 1(c). According to the SEM image, the edge length of vertical oriented ZnO NRs ranges from 50 to 80 nm and height is roughly 800 nm (shown in Fig. S2 in the supplementary material). It also can be seen that Au NPs are distributed on the top of the hexagonal shape ZnO NRs. The inset in Fig. 1(c) shows an enlarged view of the distribution of Au NP with a diameter of 10 nm. Low magnification SEM photos of pristine ZnO NRs are shown in Fig. S2 in the supplementary material.

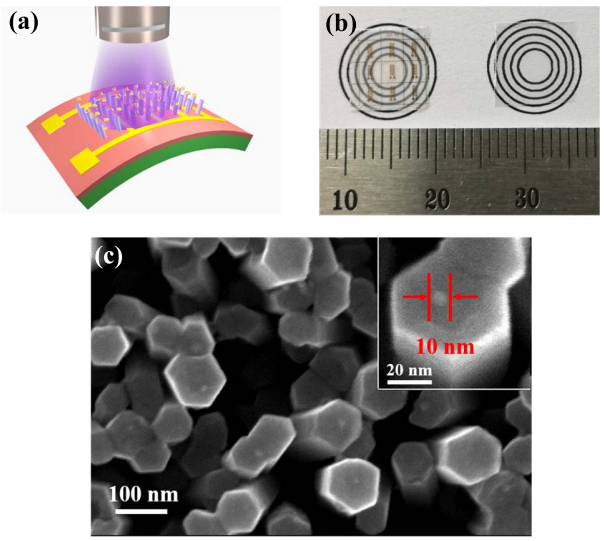

FIGURE 1. (a) Schematic of the developed Au NPs-decorated ZnO NRs UV photodetector. (b) Optical image of the fabricated devices (left) and mica substrate (right) on the paper with circular patterns. (c) FESEM image of Au NPs decorated ZnO NRs. The inset in Fig. 1(c) is the partially enlarged view of ZnO NRs decorated with Au NPs.

In this study, X-ray diffraction (XRD) analysis was performed to determine the crystal orientation of ZnO NRs. Since mica substrate shows several strong diffraction peaks which will submerge diffraction peaks of the ZnO NRs, silicon was used as the growth substrate of the ZnO NRs in the experiment instead of mica. The XRD peaks of the ZnO NRs grown on the mica substrate is shown in Fig. S3 in the supplementary material. Fig. 2(a) depicts the XRD patterns of pristine ZnO NRs and Au NPs decorated ZnO NRs. The XRD patterns of all the samples showed two peaks. One of the peaks comes from the silicon substrate and the other peak is at 34.5°, corresponding to the hexagonal wurtzite (002). These results reveals that no other related phases have been formed. Fig. 2(b) shows the photoluminescence (PL) spectra of pristine and Au NPs decorated ZnO NRs excited by a He-Cd laser with 325 nm wavelength. It can be clearly seen that both two different types of ZnO NRs show two emission peaks regardless of whether they are modified by Au NPs or not. One of the peaks is located at approximately 385 nm, which is due to the inter-band recombination of ZnO NRs. The other peak is in the visible region ranging from 450 to 700 nm, which is mainly caused by deep-level defects. These deep-level defects in ZnO NRs mainly come from oxygen vacancies and zinc interstitials [18], [19]. It is worth noting that the ZnO NRs with Au NPs emit a lower broadband signal in the visible range, indicating that the Au NPs suppress the broadband emission. At the same time, the emission peak related to inter-band recombination of ZnO NRs with Au NPs is greatly improved compared to that of the pristine ZnO NRs and these results are consistent with the previous works [20]–[24]. Therefore, it can be seen from the PL spectrum results that the Au NPs distributed on the surface of the ZnO NRs can passivate the surface defects of the material and ultimately improve the optical properties of the ZnO NRs. These two differences are mainly due to the LSPR effect of Au NPs which will be discussed later. UV-visible spectra of ZnO NRs and Au NPs solution are shown in Fig. 2(c) and (d), respectively. The spectrum of Au NPs decorated ZnO NRs clearly shows two peaks: one at the 380 nm UV band and the other in the visible region (530 nm). The peak in the UV region is mainly from the bandedge absorption of ZnO NRs and that in the visible region is due to the surface plasmon absorption of Au NPs, which is the characteristic peak of Au NPs of average size ∼10 nm [25]–[27]. Therefore, the small hump that appears in the absorption spectrum of ZnO NRs with Au NPs decorated in the inset of Fig. 2(c) at ∼530 nm can be assigned to the Au NPs.

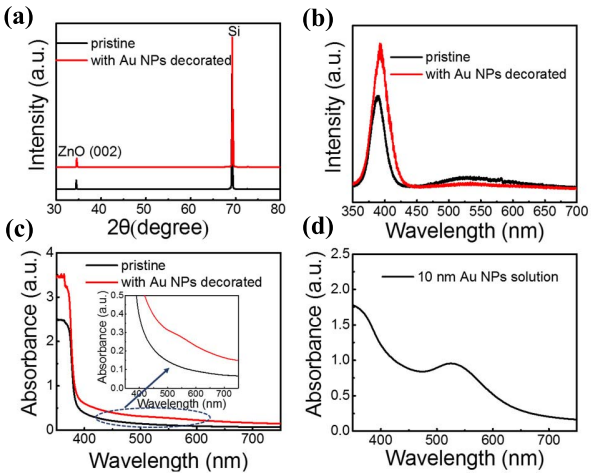

FIGURE 2. (a) XRD patterns of pristine and Au NPs-decorated ZnO NRs. (b) Room temperature photoluminescence spectra of pristine (black line) and Au NPs decorated (red line) ZnO NRs. (c) UV–Vis absorption spectrum of pristine (black line) and Au NPs decorated (red line) ZnO NRs. The inset in Fig. 2(c) is the illustration of partial enlargement of UV-Vis absorption spectrum. (d) UV–Vis absorption spectrum of 10 nm Au NPs solution.

The schematics of the fabrication steps involved during the fabrication of the photodetectors are illustrated in Fig. S4 in the supplementary material. The current-voltage (I-V) characteristics of the photodetectors for pristine and Au

NPs decorated ZnO NRs under dark condition and different light power intensities, are shown in Fig. 3(a) and 3(b), respectively. Under dark condition, oxygen molecules will be adsorbed on the surface of ZnO NRs and capture free electrons. Such a reaction process on the surface can be described as follows [28]:

$$\frac{1}{2}O_{2(g)} + 2e^{2-} = O^{2-}_{(ad)} \tag{1}$$

In addition to this, since the work functions of the two materials are different, electrons will flow from the ZnO NRs side to the Au NPs side. When the Fermi energy level of the materials on both sides becomes the same, a Schottky barrier is formed at the interface between the ZnO NRs and the Au NPs. When the photon energy of the UV illumination was larger than the band gap of ZnO, the electrons will transit from the valence band to the conduction band, generating electron-hole pairs. The photogenerated holes migrate to the ZnO NRs surface and desorb the oxygen ions by surface electron-hole recombination. Therefore, the remaining photogenerated electrons increase the conductivity of ZnO NRs. The surface desorption reactions during the photocurrent growth can be described as follow [29]:

$$h\nu \rightarrow e^- + h^+ \tag{2}$$

$$2h^+ + O^{2-}_{(ad)} = O_{(g)} \tag{3}$$

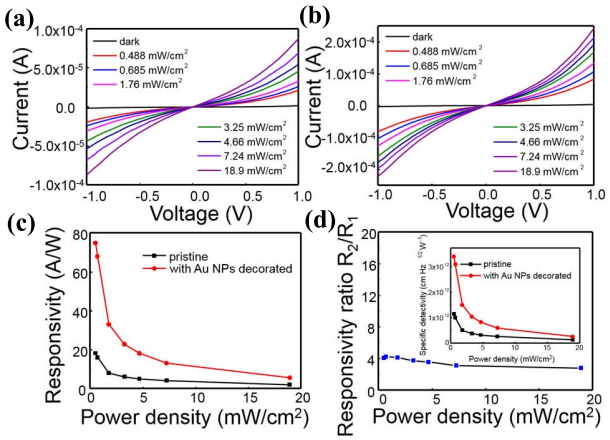

FIGURE 3. (a) - (b) The measured I-V characteristics of the photodetectors for pristine ZnO NRs and Au NPs decorated ZnO NRs under dark condition and different light power illumination intensities. (c) The calculated responsivity of photodetector under different light power densities. (d) The enhancement factor of responsivity versus light power density for the devices. The inset in Fig. 3(d) is the calculated specific detectivity of photodetector under different light power densities. The illumination wavelength is 365 nm.

In the experiment, 365 nm ultraviolet light was used to calibrate the UV performance of the photodetector. In order to assess the performance of the device, two important parameters such as responsivity (R_λ) and specific detectivity (D_λ*) at −1V external bias voltage at 365 nm wavelength was calculated by the following formula:

$$R_\lambda = \frac{I_p - I_d}{P_d \cdot S} \tag{4}$$

$$D^*_\lambda = \frac{R \cdot \sqrt{S}}{\sqrt{2qI_d}} \tag{5}$$

where I_p and I_d are the photocurrent and dark current, P_d is the optical power density, S is the effective area of the device, q is the electronic charge. With the introduction of Au NPs decorated, the UV responsivity and specific detectivity reached 70 A/W and 3.41 × 10^{12} cm $Hz^{1/2}$ W^{-1}, respectively, which were enhanced by approximately 4 times at an excitation wavelength of 365 nm compared with those of pristine ZnO NRs. It can be seen from Fig. 3(c) and (d) that although the UV responsivity of the device decreases as light power density increases, the responsivity enhancement factor, defined as the ratio R_2/R_1 is almost unchanged. R_2 and R_1 represents the responsivity of device of Au NPs decorated ZnO NRs and pristine ZnO NRs, respectively.

Besides enhanced optoelectric performance due to the decoration of Au NPs, the UV photodetector fabricated in this work also shows some other preferable properties. ZnO NRs has great application potential in flexible photodetectors [30]–[33] and benefiting from the good flexibility of mica substrate [34], flexible photodetectors based on ZnO NRs were fabricated on mica substrate by traditional device fabrication process. The in situ bending test of the device are shown in Fig. 4(a) and (b). The device was fixed on a metal holder and bent to a fixed bending radius of curvature to test its performance. The setup of fatigue test is demonstrated in Fig. 4(c) and (d) and this setup allows the devices to bend and stretch periodically to different degrees. Combined with the excellent flexible and bendable performance of mica substrate, the photoresponse of the device with Au NPs decorated under different bending radii of curvature (R = 8, 7, and 6 mm) with 365 nm wavelength were well maintained compared with that of device under flat condition as shown in Fig. 4(e), indicating that bending stress can hardly influence the photoelectric performance of the device. The I-V characteristics of photodetector for Au NPs decorated ZnO NRs with different bending radii of curvature (R = 8, 7 and 6 mm) are revealed in Fig. S5 in the supplementary material. We could also clearly observe that after bending 200 cycles (with average bending radius of curvature 8 mm), the photocurrent of the device has almost unchanged revealing that the flexible ZnO NRs based photodetector has good fatigue resistance to bending. It also can be clearly seen from Fig. 4(f) that although the UV responsivity of the device decreases as light power density increases, the responsivity enhancement factor, defined as the ratio R_3/R_1 is almost unchanged. R_3 and R_1 represents the responsivity of device of Au NPs decorated ZnO NRs (under flat or different bending radii of curvature) and pristine ZnO NRs, respectively. Furthermore, the current response of the device was also tested and the results are shown in Fig. 4(g) and (h). The periodic current-time (I-T) photoresponse test results reveal the high repeatability at −1V bias voltage with a low illumination intensity of 3.25 mW cm^{-2} at 365 nm wavelength. These results clearly demonstrate the excellent

photoelectric stability of this device under extreme bending conditions.

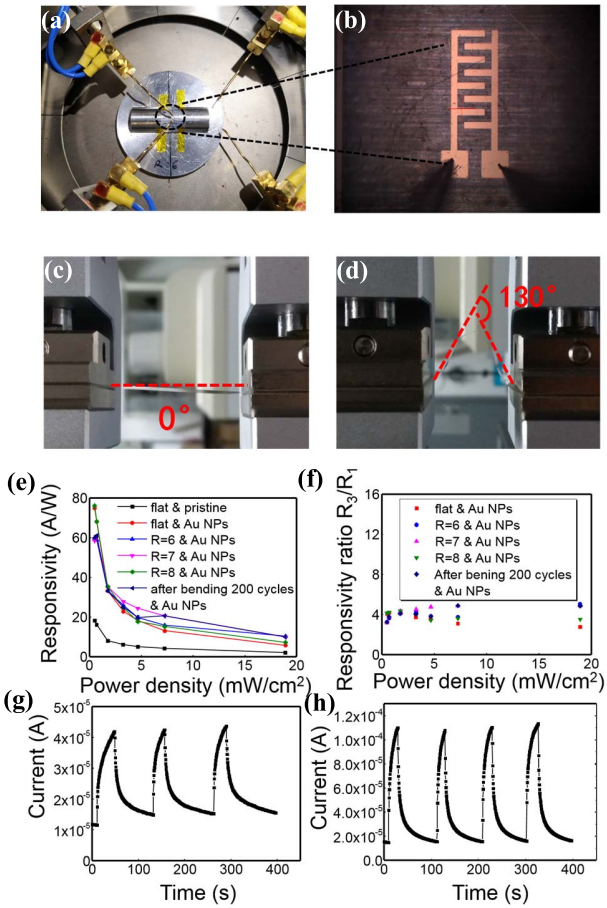

FIGURE 4. (a) Setup image of bending test in situ of device. (b) Optical image of bending test in situ. (c) - (d) Fatigue performance test setup with different bending degrees. (e) The calculated responsivity and (f) enhancement factor of responsivity versus light power density of the device with different bending radii of curvature and 200 bending cycles. (g) - (h) The I-T response of the device for pristine and Au NPs decorated ZnO NRs, respectively. The illumination wavelength is 365 nm.

The flexibility, combined with the mechanical stability of the device, enables it to be attached to surfaces of various shapes. This allows the device to be used in narrow holes, sharp corners, or other places which is hard to access by traditional rigid photodetectors. Also, the device has a potential to be applied in wearable electronic devices. Another property of the device is its transparency. The mica substrate, as suggested by Fig. 1(b), has very low optical absorption and reflection in the wavelength range of visible light and we can clearly see the patterns under the device which confirms the excellent transparency. All these characteristics indicate that such phtotodetector has a great potential for application in manufacturing flexible and transparent integrated optoelectronics.

In order to better understand the surface plasmon coupling between Au NPs and ZnO NRs, an energy band structure diagram is illustrated in Fig. 5(a) to explain the enhancement

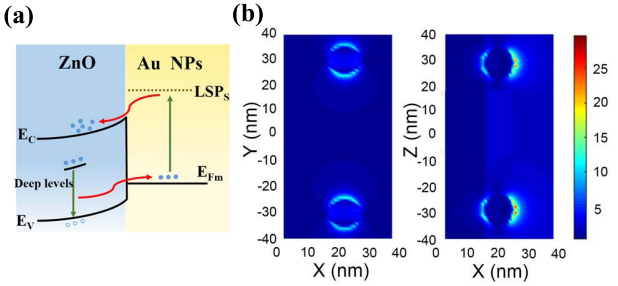

FIGURE 5. (a) Band-diagram of Au NPs/n-ZnO NRs used to elucidate the surface plasmon coupling between Au NPs and ZnO NRs. (b) The electric field profiles of ZnO NRs with Au NPs on the top surface (left) and sidewall (right) from FDTD simulation, respectively.

of UV response. For pristine ZnO NRs, there are a large amount of defects on its surface which can lead to some defect-related emission in the visible band. When the Au NPs solution was sprayed onto the surface of the ZnO NRs, the broadband emissions are suppressed and electrons in the defect level of ZnO NRs can easily flow into the Au NPs since the Fermi level of Au is very close to the defect level of ZnO [35], [36]. From the previous study [12]–[16], the resonance position of Au NPs localized surface plasmons (SPs) is consistent with the range of the defect-related green emission of ZnO NRs. Therefore, the green emission can excite the localized SPs in Au NPs. To further explain the previous experimental results, the FDTD simulations are performed to calculated electric distribution. The simulation is simplified by several Au NPs with a diameter of 10 nm attached to the surface of ZnO NRs according to the above SEM results. The color index represents the magnitude of the electric field intensity. The near field distribution was plotted in Fig. 5(b) showing that whether on the top or on the side of the ZnO NRs, the near field intensity ($|E|^2$) around the Au NPs were enhanced by approximately several times than that of pristine ZnO NRs under 530 nm illumination. This significant enhancement of the near field intensity is due to LSPR of the Au NPs. According to previous studies, the Schottky barrier height (SBH) at the interface between Au NPs and ZnO NRs is about 0.6 - 0.8 eV [21], [37]. The resonance energy range of Au NPs is between 1.9 −2.6 eV (corresponding to the 480∼650 nm wavelengths) which is much higher than the SBH of 0.6 - 0.8 eV between the Au NPs/ZnO NRs interface. The near field intensity was so high that it can easily pump the electrons into the conduction band of ZnO, thereby contributing to the enhancement of the photoresponse at 365 nm wavelength.

IV. CONCLUSION

In summary, Au NPs-decorated, highly oriented ZnO NRs were successfully fabricated on flexible transparent mica substrate using a simple and low-cost hydrothermal method. The introduction of Au NPs modification enhances the UV emission while suppressing of defect-related emission compared with that of pristine ZnO NRs. Due the implementation of Au NPs, the UV responsivity and specific detectivity of the

device reached 70 A/W and 3.41 $\times$ 10^{12} cm $Hz^{1/2}$ W^{-1}, respectively, which were enhanced by approximately 4 times at an excitation wavelength of 365 nm compared with those of pristine ZnO NRs. Moreover, these photodetectors fabricated on flexible mica substrate shows a stable and repeatable photoresponse even after 200 cycles bending test, indicating excellent photoelectrical and mechanical stability. We expect this study to improve understanding of plasmon induced charge-transfer processes at the metal-semiconductor interface and eventually would be beneficial to the development of future high responsivity, low cost and flexible ZnO NRs based UV optoelectronic devices.

REFERENCES

[1] D. Gedamu *et al.*, "Rapid fabrication technique for interpenetrated ZnO nanotetrapod networks for fast UV sensors," *Adv. Mater.*, vol. 26, no. 10, pp. 1541–1550, 2014.
[2] S.-J. Young and Y.-H. Liu, "Ultraviolet photodetectors with 2-D indium-doped ZnO nanostructures," *IEEE Trans. Electron Devices*, vol. 63, no. 8, pp. 3160–3164, Aug. 2016.
[3] Y.-H. Liu, S.-J. Young, L.-W. Ji, and S.-J. Chang, "Ga-doped ZnO nanosheet structure-based ultraviolet photodetector by low-temperature aqueous solution method," *IEEE Trans. Electron Devices*, vol. 62, no. 9, pp. 2924–2927, Sep. 2015.
[4] C.-L. Hsu and S.-J. Chang, "Doped ZnO 1D nanostructures: Synthesis, properties, and photodetector application," *Small*, vol. 10, no. 22, pp. 4562–4585, 2015.
[5] X. Q. Meng, H. Peng, Y. Q. Gai, and J. Li, "Influence of ZnS and MgO shell on the photoluminescence properties of ZnO core/shell nanowires," *J. Phys. Chem. C*, vol. 114, no. 3, pp. 1467–1471, 2010.
[6] J. Song *et al.*, "Investigation of enhanced ultraviolet emission from different Ti-capped ZnO structures via surface passivation and surface plasmon coupling," *Appl. Phys. Lett.*, vol. 97, no. 12, 2010, Art. no. 122103.
[7] D. Zhao *et al.*, "Surface modification effect on photoluminescence of individual ZnO nanorods with different diameters," *Nanoscale*, vol. 5, no. 10, pp. 4443–4448, 2013.
[8] J. P. Richters, T. Voss, D. S. Kim, R. Scholz, and M. Zacharias, "Enhanced surface-excitonic emission in ZnO/Al_2O_3 core-shell nanowires," *Nanotechnology*, vol. 19, no. 30, pp. 11600–11608, 2008.
[9] T. Dixit, I. A. Palani, and V. Singh, "Role of surface plasmon decay mediated hot carriers towards the photoluminescence tuning of metal coated ZnO nanorods," *J. Phys. Chem. C*, vol. 121, no. 6, pp. 3540–3548, 2017.
[10] S. T. Kochuveedu, Y. H. Jang, and D. H. Kim, "A study on the mechanism for the interaction of light with noble metal-metal oxide semiconductor nanostructures for various photophysical applications," *Chem. Soc. Rev.*, vol. 42, no. 21, pp. 8467–8493, 2014.
[11] A. Pescaglini *et al.*, "Hot-electron injection in Au nanorod-ZnO nanowire hybrid device for near-infrared photodetection," *Nano Lett.*, vol. 14, no. 11, pp. 6202–6209, 2014.
[12] M. M. Brewster, X. Zhou, S. K. Lim, and S. Gradečak, "Role of Au in the growth and nanoscale optical properties of ZnO nanowires," *J. Phys. Chem. Lett.*, vol. 2, no. 6, pp. 586–591, 2011.
[13] J. M. Lin, H. Y. Lin, C. L. Cheng, and Y. F. Chen, "Giant enhancement of bandgap emission of ZnO nanorods by platinum nanoparticles," *Nanotechnology*, vol. 17, no. 17, pp. 4391–4394, 2006.
[14] M. K. Lee, T. G. Kim, W. Kim, and Y. M. Sung, "Surface plasmon resonance (SPR) electron and energy transfer in noble metal-zinc oxide composite nanocrystals," *J. Phys. Chem. C*, vol. 112, no. 27, pp. 10079–10082, 2008.
[15] J. Im, J. Singh, J. W. Soares, D. M. Steeves, and J. E. Whitten, "Synthesis and optical properties of dithiol-linked ZnO/gold nanoparticle composites," *J. Phys. Chem. C*, vol. 115, no. 21, pp. 10518–10523, 2011.
[16] J. Lu *et al.*, "Improved UV photoresponse of ZnO nanorod arrays by resonant coupling with surface plasmons of Al nanoparticles," *Nanoscale*, vol. 7, no. 8, pp. 3396–3403, 2015.
[17] F. F. Qin *et al.*, "Extra green light induced ZnO ultraviolet lasing enhancement assisted by Au surface plasmons," *Nanoscale*, vol. 10, no. 2, pp. 623–627, 2018.
[18] H. Y. Lin *et al.*, "Enhancement of band gap emission stimulated by defect loss," *Opt. Exp.*, vol. 14, no. 6, pp. 2372–2379, 2006.
[19] K. Wu *et al.*, "Enhanced near band edge emission of ZnO via surface plasmon resonance of aluminum nanoparticles," *J. Appl. Phys.*, vol. 110, no. 2, 2011, Art. no. 023510.
[20] R. Khan, J.-H. Yun, K.-B. Bae, and I.-H. Lee, "Enhanced photoluminescence of ZnO nanorods via coupling with localized surface plasmon of Au nanoparticles," *J. Alloys Compounds*, vol. 682, pp. 643–646, Oct. 2016.
[21] J. D. Hwang, F. H. Wang, C. Y. Kung, and M. C. Chan, "Using the surface plasmon resonance of Au nanoparticles to enhance ultraviolet response of ZnO nanorods-based Schottky-barrier photodetectors," *IEEE Trans. Nanotechnol.*, vol. 14, no. 2, pp. 318–321, Mar. 2015.
[22] J.-D. Hwang, M. J. Lai, H. Z. Chen, and M. C. Kao, "Au-mediated surface plasmon enhanced ultraviolet response of p-Si/n-ZnO nanorods photodetectors," *IEEE Photon. Technol. Lett.*, vol. 26, no. 10, pp. 1023–1026, May 15, 2014.
[23] T.-C. Chiang, C.-Y. Chiu, T.-F. Dai, Y.-J. Hung, and H.-C. Hsu, "Surface-plasmon-enhanced band-edge emission and lasing behaviors of Au-decorated ZnO microstructures," *Opt. Mater. Exp.*, vol. 7, no. 2, pp. 313–319, 2017.
[24] C. W. Cheng *et al.*, "Surface plasmon enhanced band edge luminescence of ZnO nanorods by capping Au nanoparticles," *Appl. Phys. Lett.*, vol. 96, no. 7, 2010, Art. no. 071107.
[25] S. Link and M. A. El-Sayed, "Size and temperature dependence of the plasmon absorption of colloidal gold nanoparticles," *J. Phys. Chem. B*, vol. 103, no. 21, pp. 4212–4217, 1999.
[26] B. Balamurugan and T. Maruyama, "Evidence of an enhanced interband absorption in Au nanoparticles: Size-dependent electronic structure and optical properties," *Appl. Phys. Lett.*, vol. 87, no. 14, 2005, Art. no. 143105.
[27] P. K. Jain, X. Huang, I. H. El-Sayed, and M. A. El-Sayed, "Review of some interesting surface plasmon resonance-enhanced properties of noble metal nanoparticles and their applications to biosystems," *Plasmonics*, vol. 2, no. 3, pp. 107–118, 2007.
[28] S. Y. Bae, C. W. Na, J. H. Kang, and J. Park, "Comparative structure and optical properties of Ga-, In-, and Sn-doped ZnO nanowires synthesized via thermal evaporation," *J. Phys. Chem. B*, vol. 109, no. 7, pp. 2526–2531, 2005.
[29] Y. Li, F. D. Valle, M. Simonnet, I. Yamada, and J.-J. Delaunay, "Competitive surface effects of oxygen and water on UV photoresponse of ZnO nanowires," *Appl. Phys. Lett.*, vol. 94, no. 2, 2009, Art. no. 023110.
[30] G. Jang *et al.*, "Flexible UV detector based on carbon fibers, ZnO nanorods, and Ag nanowires," *J. Mater. Chem. C*, vol. 5, no. 18, pp. 4537–4542, 2017.
[31] V. Q. Dang *et al.*, "High-performance flexible ultraviolet (UV) phototransistor using hybrid channel of vertical ZnO nanorods and graphene," *ACS Appl. Mater. Interfaces*, vol. 7, no. 20, pp. 11032–11040, 2015.
[32] I.-C. Yao, T.-Y. Tseng, and P. Lin, "ZnO nanorods grown on polymer substrates as UV photodetectors," *Sensors Actuators A Phys.*, vol. 178, pp. 26–31, May 2012.
[33] T. P. Chen, S.-J. Young, S. J. Chang, and C. H. Hsiao, "Photoconductive gain of vertical ZnO nanorods on flexible polyimide substrate by low-temperature process," *IEEE Sensors J.*, vol. 11, no. 12, pp. 3457–3461, Dec. 2011.
[34] D. Y. Kim *et al.*, "High temperature processed ZnO nanorods using flexible and transparent mica substrates for dye-sensitized solar cells and piezoelectric nanogenerators," *Nano Energy*, vol. 9, pp. 101–111, Oct. 2014.
[35] S. G. Zhang *et al.*, "Plasmon-enhanced ultraviolet photoluminescence from highly ordered ZnO nanorods/graphene hybrid structure decorated with Au nanospheres," *J. Phys. D Appl. Phys.*, vol. 47, no. 49, pp. 495103–495108, 2014.
[36] R. Liu *et al.*, "Graphene plasmon enhanced photoluminescence in ZnO microwires," *Nanoscale*, vol. 5, no. 12, pp. 5294–5298, 2013.
[37] J.-D. Hwang, C.-Y. Kung, and Y.-L. Lin, "Non-surface-treated Au/ZnO Schottky diodes using pre-annealed hydrothermal or sol-gel seed layer," *IEEE Trans. Nanotechnol.*, vol. 12, no. 1, pp. 35–39, Jan. 2013.

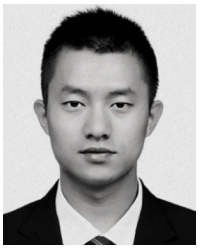

HAINAN ZHANG received the bachelor's degree from the Harbin Institute of Technology in 2016. He is currently pursuing the Ph.D. degree with Tsinghua University, Beijing.

He currently concentrates on the research topics on novel 2-D materials and wide bandgap semiconductor-based photodetector.

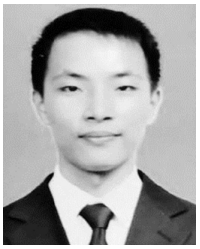

YUNFEI ZHAO received the bachelor's degree in materials science and engineering from Tsinghua University, Beijing, China, in 2012 and the master's and Ph.D. degrees from Iowa State University, Ames, IA, USA, in 2014 and 2017, respectively. He is currently a Post-Doctoral Fellow with the Institute of Microelectronics, Tsinghua University.

His current research interests are PZT and ZnO-based flexible ultrasonic transducer arrays, ZnO-based ultraviolet photodetectors, and graphene-based devices.

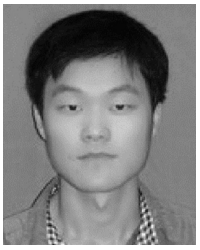

XIANGSHUN GENG received the master's degree in electronic science and technology from the Hefei University of Technology, Hefei, China, in 2017. He is currently pursuing the Ph.D. degree with the Institute of Microelectronics, Tsinghua University.

His current research area concentrates on novel materials and photoelectronic devices.

YAO HUANG received the bachelor's degree in electronic science and technology from Northwestern Polytechnical University, Xi'an, China, in 2018. She is currently pursuing the master's degree in IC engineering with Tsinghua University.

Her current research interests are ZnO nanorods and UV photodetector.

YUXING LI received the bachelor's degree in electronic science and technology from Tsinghua University, Beijing, China, in 2014, where he is currently pursuing the Ph.D. degree in electronics science and technology.

His current research interests are Hafnia-based ferroelectric films, thin film transistor, and novel 2-D materials.

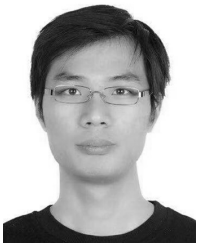

HOUFANG LIU received the B.S. degree in physics from Shandong University and the Ph.D. degree in condensed matter physics from the Institute of Physics, Chinese Academy of Sciences, Beijing, China, in 2013.

His current research interest includes spintronics with 2-D materials, magnetoresistance effect, and nonvolatile RAM.

YU LIU received the B.E. degree in microelectronics from the University of Electronic Science and Technology of China in 2017. He is currently pursuing the Ph.D. degree with the Institute of Microelectronics, Tsinghua University.

His research concentrates on the fabrication and fundamental physics of novel electronic/optoelectronic devices.

YUTAO LI received the bachelor's degree in electronic science and technology from the Huazhong University of Science and Technology, Wuhan, China, in 2015. He is currently pursuing the Ph.D. degree in science and technology with Tsinghua University, Beijing, China.

His current research interests are novel micro-nano optoelectronic device, carbon nano material, and novel 2-D material.

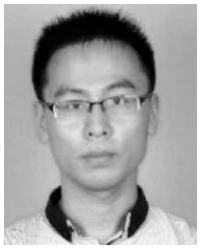

XUEFENG WANG received the bachelor's degree from Shandong University, Jinan, in 2014. He is currently pursuing the Ph.D. degree with Tsinghua University, Beijing.

He currently concentrates on the research topics on new 2-D materials devices, resistive memory, and synaptic transistor.

HE TIAN received the Ph.D. degree from the Institute of Microelectronics, Tsinghua University, in 2015, where he is currently an Assistant Professor. He was a recipient of the IEEE EDS Ph.D. Student Fellowship and Tsinghua University Top-Ten Scholarship in 2013.

He has co-authored over 100 papers and has over 1500 citations. He has been researching on various 2-D material-based novel nanodevices.

RENRONG LIANG received the Ph.D. degree in electronics science and technology from Tsinghua University, Beijing, China, in 2008, where he has been an Assistant Professor with the Institute of Microelectronics since 2010.

His current research interests are concerned with fabrication and simulation of SiGe and 2-D materialsbased devices, transport models and optimization of low-power nanoscale MOS devices, such as strained Si MOSFETs, FinFETs, tunneling FETs and negative capacitance FETs, and device physics.

TIAN-LING REN received the Ph.D. degree in solid-state physics from the Department of Modern Applied Physics, Tsinghua University, Beijing, China, in 1997, where he has been a Full Professor with the Institute of Microelectronics since 2003.

His main research interests include 2-D-material-based devices and novel nanoelectronic devices, intelligent sensors and integrated micro-electromechanical systems, and critical technology for advanced micro- and nano-electronics.